

CORROSION ASSESSMENT IN KARAN GAS FIELD DEVELOPMENT

Marc Singer⁽¹⁾, Srdjan Nestic,
Ohio University - Institute for Corrosion and Multiphase Technology
342 West State St., Athens, OHIO, 45701

Jamal N. Al-Khamis
Saudi Arabian Oil Company
PO Box 12262 Dhahran 31311 Saudi Arabia

ABSTRACT

The Karan offshore development is expected to produce a large quantity of natural gas but no hydrocarbon condensate. Liquid water is, however, projected to be present through condensation and the presence of CO₂ (8%) and H₂S (4%) will lead to aggressive corrosion environments. Different inhibition techniques will be implemented to control bottom of the line corrosion. Top of the line corrosion (TLC) is also a potential issue in specific locations in the field as large quantities of organic acids are present in the produced water. This paper presents a comprehensive assessment of the corrosion risk through laboratory simulations performed in a large scale flow loop as well as in a specially designed autoclave equipped for corrosion studies under dewing conditions. Corrosion rates are obtained through weight loss methods and the surface layer is analysed with XRD (X-ray diffraction), EDS (Energy Dispersive Spectroscopy) and SEM (Scanning Electron Microscopy). The TLC rate was found to be low in all conditions tested and no indications of localized corrosion was observed. Mackinawite, cubic iron sulfide, and troilite (stoichiometric pyrrhotite) were identified in the corrosion product layer. The results are used to guide the required corrosion management measures, which are also presented.

KEYWORDS: Top of the line corrosion, H₂S, CO₂, Water condensation rate.

BACKGROUND**Field description**

The Karan development is the first offshore gas production facility for Saudi Aramco⁽²⁾. The Karan field will be located 80–100 km offshore at a 50–60 meter depth in the Gulf (Figure 1). The development will initially comprise of four wellhead production platforms each functioning unmanned to receive, commingle and export up to 500 MMSCFD of gas from a number of production wells to one central Tie-In Platform (TP) via 20in flowlines (1.1 – 7 km in length). A single 38in, 110 km trunkline will transport the wet produced gas from the TP to the onshore gas processing facility. Out of the 110 km, 85 km is offshore, and the remaining 25 km is onshore. The field is targeted for producing about 1,800 MMSCFD. The gas is lean with no hydrocarbon condensate dropping out in the planned operational region.

The gas has approximately 8.5 mol% CO₂, 2 mol% H₂S, 1350 ng/m³ Hg, and 750 ppm of organic acids. Estimated water production is about 2 barrels of condensed water per MMSCFD, with no produced water anticipated throughout the first 20 years of production.

(1) Corresponding author. Email address: singer@ohio.edu

(2) Author's company name

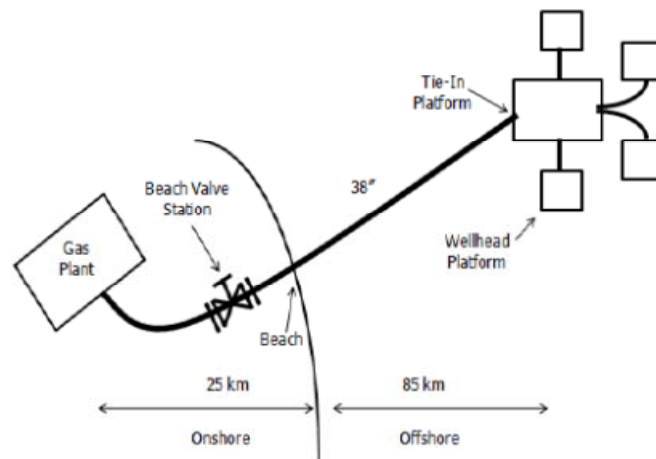


Figure 1: Schematic of the Karan Field Development

Identification of corrosion or production issues

In offshore wet sour gas production with long pipelines, hydrate and corrosion inhibition is required and essential in order to ensure safe, reliable and cost-effective operations. With the identified operating conditions, corrosion will become a major concern for the operation of Karan facilities. Identifying the nature of the anticipated corrosion processes is a key to determining the major components of any future corrosion management program.

In particular, top of the line corrosion (TLC) was identified as a potential issue in specific locations in the field as large quantities of organic acids are present in the condensed water. TLC occurs when the surrounding environment cools down the produced gas that is saturated with water vapor. As the gas is cooled, the water vapor in the gas will condense. When this happens, corrosion can occur. This type of corrosion has not been experienced by the author's company. However, other offshore gas producers around the world have experienced this problem.

To help identify the corrosion challenges for this field, the author's company initiated in 2008 a comprehensive study to determine the likelihood and extent of different corrosion mechanisms at such conditions.

The first experimental tests were aimed at simulating the field conditions. They included:

- Long-term tests in the large layer H₂S loop. This test reproduced the flow regime and the H₂S/CO₂ ratio observed in the field conditions but not the real partial pressure of H₂S.
- A series of long-term autoclave tests (in a simplified setup). These tests reproduced the correct H₂S/CO₂ ratio partial pressure of H₂S observed in the field but the fluid was stagnant.

The results related to these two series of experiments are presented in this paper.

Corrosion mitigation approach

Based on the benchmarking efforts with offshore gas producers around the world, a number of options have been evaluated for Karan pipelines. Bare carbon steel with inhibition similar to some gas fields operating in the Gulf was considered. To adequately protect the top of the line against corrosion, frequent batch inhibition treatment (monthly) will be required. This treatment requires running the scraper train at a low speed which will also impact the gas deliverability. This operation is also manpower intensive and will be expensive for unmanned facilities. Another option is to use alloy cladding. This is not only a much more expensive option, but also has about a 2 year delay on the project due to delivery of materials. Accordingly, the following mitigation measures were recommended:

- Use of UNS N08028 for the well tubing
- Use of UNS N06625 Cladding for the wellhead and topside piping

Aside from being cost effective, the recommended option has other benefits. It affords the needed corrosion protection. Less batch treatment will be required from monthly to quarterly or semi-annually. Inhibitor dosage would be much less. Internal coating will be done locally. Corrosion inhibitor solution will also be blended locally.

LABORATORY STUDY ON SOUR TLC

Introduction

Top of the line corrosion is a type of corrosion which happens in stratified flow when strong gradients of temperature between the outside environment and the process fluid lead to water condensation on the internal walls of the pipe line. It was first identified in the '60s¹ and is now a growing concern for the oil and gas industry. Many field cases have been published since, both for onshore and offshore production environments²⁻⁹. The presence of the condensed water can induce severe problems of general corrosion and pitting typically on the upper part of the pipe (between 9 and 3 o'clock).

There are two different categories of TLC depending on whether TLC is dominated by CO₂ or H₂S. Top of the line corrosion in sweet (CO₂) conditions depends mostly on the condensation rate, the gas temperature, the gas flow rate, the CO₂ partial pressure and the presence of organic acid. Pipe inspections often reveal corrosion over extended areas of the top of the pipeline associated with breakdowns of an otherwise protective FeCO₃ layer. Experimental and field experience in this domain is growing and a lot of research work has been already published¹⁰⁻¹⁵.

In sour conditions, the mechanism governing top of the line corrosion seems largely different from sweet conditions. Several field failures attributed to sour TLC have been reported^{1,5-9} although sour TLC does not seem to be as serious and as common as in sweet TLC. Limited research work has been published so far on sour TLC¹⁶⁻¹⁸ leading often to more experimental interrogation than real answers. It seems that the controlling parameters are related to the protectiveness of the corrosion product layer which should be mostly dependent on the fluid temperature, pH and the iron ion content.

Extensive experimental work performed for multiphase bottom of the line conditions showed a subsequent reduction of the corrosion rate compared to a baseline pure CO₂ environment when small amounts of H₂S were introduced¹⁹⁻²³. This is associated with the formation of a protective mackinawite film. However, different environmental conditions can lead to the formation of various thermodynamically stable types of FeS²⁴ and, consequently, various scenarios of corrosion. However, the link between the types of FeS formed and their specific protectiveness has not been adequately established yet. The presence of organic acids, so harmful to TLC in sweet environments¹⁰, has been reported to greatly affect the protectiveness of mackinawite as well and lead to localized corrosion in bottom of the line corrosion²⁵ scenarios and is thought to also play a role in sour TLC.

Objectives

The main goal of this study is to simulate as closely as possible the Karan field conditions in order to evaluate the likelihood of Top of the Line Corrosion and to collect useful information about general and localized TLC rates.

In order to simulate the sour gas field environment, the thermo-hydrodynamics and the chemistry of the field conditions have to be closely matched. While the large scale loops are fully equipped for realistic TLC investigation, they are limited in terms of H₂S content due to the safety concerns associated with the presence of large quantities of toxic gas. On the other hand, autoclaves have been used to successfully conduct high pressure H₂S corrosion tests even if they cannot reproduce the hydrodynamics encountered in a gas pipeline. By combining tests performed in large scale loops and in autoclaves, it is believed that the different aspects of the wet gas field case could be closely investigated. Each test was carried out for 3 weeks and a variety of corrosion monitoring techniques were used to quantify the extent of Top of the Line Corrosion. A summary of the range of conditions tested is displayed in Table 1.

Table 1: Large scale flow loop versus autoclave

Large scale loop tests: <ul style="list-style-type: none"> • Total pressure: 3 bars • H₂S partial pressure: up to 0.1 bar • CO₂ partial pressure: up to 0.5 bars • CO₂/H₂S ratio: up to 5 • Flow regime: Stratified flow (gas velocity: 5 m/s) 	Autoclave tests: <ul style="list-style-type: none"> • Total pressure: 50 bars • H₂S partial pressure: up to 4 bars • CO₂ partial pressure: up to 10 bars • CO₂/H₂S ratio: up to 5 • Flow regime: Stagnant conditions
--	--

Test matrix

Table 2 presents the detailed conditions in which the flow loop tests were performed. Although the thermo-hydrodynamic effect is properly simulated, only the H₂S/CO₂ ratio is similar to the field conditions (not the actual partial pressures). The organic acid used is HAc (acetic acid).

Table 2: Tests 1 and 2 - Large scale flow loop tests - experimental conditions

Parameters	Test 1	Test 2
Absolute pressure (bar)	3	
pCO ₂ (bar)	0.5	
Gas temperature (°C)	55	
Condensation rate (mL/m ² /s)	0.25	0.05
Gas velocity (m/s)	5	
Undissociated HAc in tank (ppm)	250	350
H ₂ S partial pressure (bar)	0.1	
Steel type (coupons)	API X65	
pH (tank)	As measured (4.2)	
Test duration (weeks)	3 weeks	

Table 3 presents the experimental conditions of the large scale (20L) autoclave tests (made from UNS N10276). The objective of Test 3 is to build a link between autoclave and flow loop tests. Tests 4 to 7 more closely represent the wet gas field conditions (H₂S and CO₂ partial pressures).

Table 3: Tests 3 to 7 - Large scale (20L) autoclave - experimental conditions

Parameters	Test 3	Test 4	Test 5	Test 6	Test 7
Gas temperature (°C)	39.3	45.5	55	55	
Steel temperature (°C)	17	38.1	21.4	50	24.4
Absolute pressure (bar)	2.2	26.2	26.9	28.4	
pH ₂ S (bar)	0.11	1.99	1.24	4.29	
pCO ₂ (bar)	0.41	8.13	9.4	9.9	
CO ₂ /H ₂ S ratio	3.7	4.1	7.6	2.3	
Undissociated HAc (ppm)	350				
WCR (mL/m ² /s)	0.14	0.02	0.12	0.02	0.14

Flow loop experimental setup

The first two experiments were carried out in UNS N10276 4in ID flow loop, under multiphase stratified flow of water and a mixture of CO₂/H₂S. The flow loop setup can be divided into three main parts: the tank, the pump and the piping.

The tank is used for the liquid phase conditioning and heating. It is filled with de-ionized water. Acetic acid is added to reach the concentration requirements of the tests. A set of immersion heaters control the temperature.

- Positive displacement progressive cavity pumps and gas blowers are used to move the liquid and the gas phase.
- The 4in diameter flow piping (in the form of a closed loop) is 30 meters long and horizontally level. The test sections, where the measurements are taken, are located at least 8 meters downstream from the exit of the tank. The test sections (Figure 2) are 1.5 meters long pipe spool pieces. Each test section has up to eight probe ports (four at the top, four at the bottom). In this paper, only the top of the line results are reported. Samples of condensed liquid and *in situ* pH measurements were taken at the test section. A complete description of the procedure followed during the experimental part can be found elsewhere²⁸.



Figure 2: UNS N10276 flow loop TLC test section

Autoclave experimental setup

The autoclave tests presented in this paper were conducted in a 20L autoclave made of UNS N10276. The autoclave is specially manufactured to enable corrosion measurements under condensing conditions. The top lid of the autoclave is equipped with an internal cooling system and the sample holder plate (Figure 3). The steel samples have a diameter of 5.7 cm and are made of API X65 steel. The whole surface of the steel samples was coated with an electrical insulator except for the “face” exposed to the flowing gas phase. Prior to each test, the samples were polished using 600 grit sand paper and cleaned with isopropanol. The design of the sample holder enables the study of the effect of the various condensation rates in one single test. This was done by “hanging” some of the steel samples in the gas phase but away from the cooled plate experiencing much less condensation. The samples were not immersed in the bulk liquid phase.



Figure 3: The 20L UNS N10276 autoclave setup (left) and details of the cooled sample holder (right)

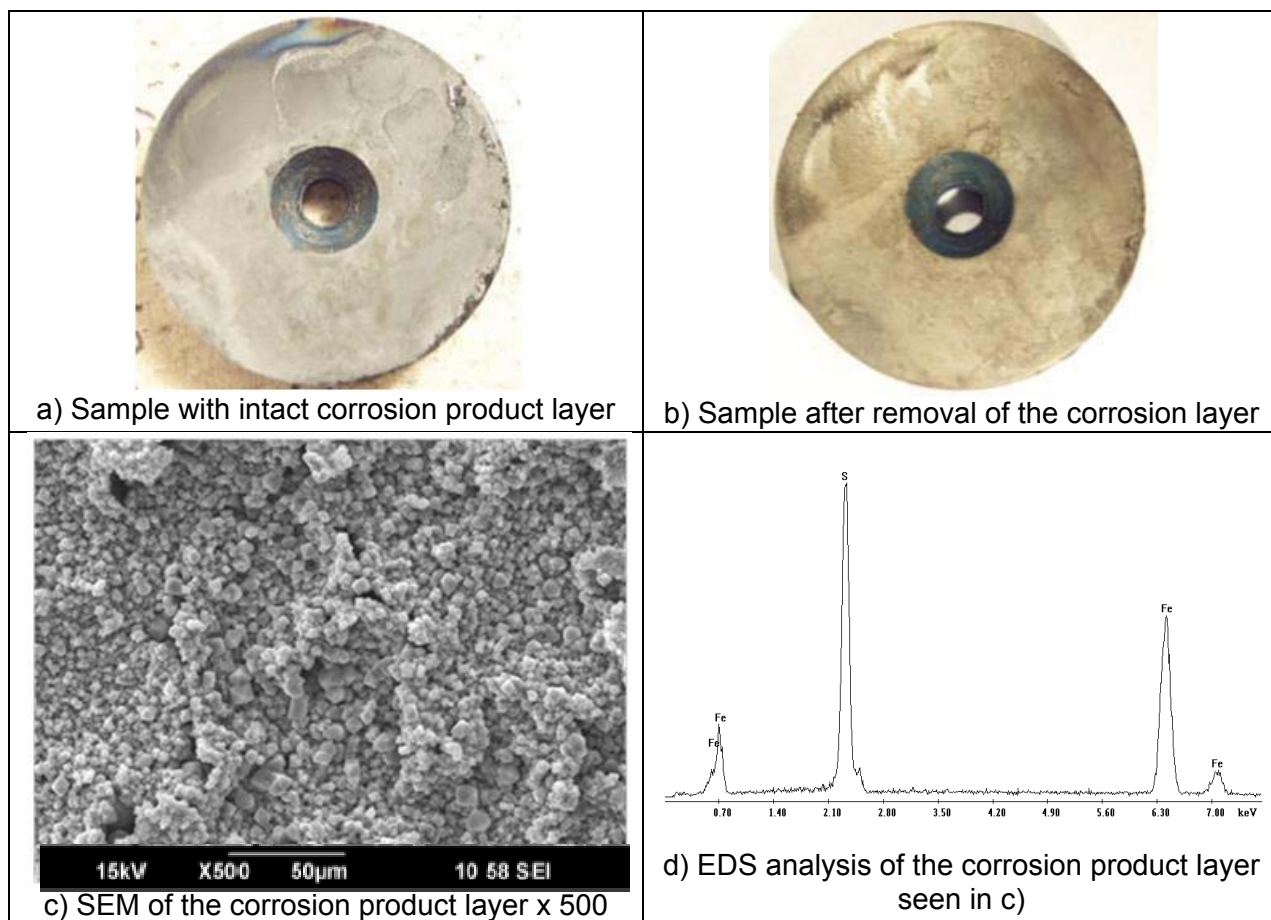
Typically, 8 litres of de-ionized water was introduced in the autoclave at the beginning of the test and de-oxygenated for two hours before the correct amount of pure acetic acid was introduced. The sample holder was then attached to the top lid and the autoclave was sealed, heated to the required temperature and pressurized with N₂ to 2 bars total pressure. Pure H₂S gas was then bubbled into the liquid until the total pressure reached a stable required reading (1.2 or 4 bars of H₂S). In the same manner, CO₂ was added to reach a partial pressure of 10 bars, and the pressure was

increased up to 25 bars with N₂. The concentration of H₂S in the gas phase was measured at the end of the test. According to calculation, the pH of the main liquid bulk solution should have remained around pH3.4-3.5 during the three weeks of testing. The temperature of the steel sample holder was measured using a thermocouple, and the water condensation was calculated using an in-house heat/mass transfer model. At the end of the test, the gas phase was purged for a few hours with nitrogen before opening the autoclave and removing the steel samples. A liquid sample was then taken for acetic acid analysis. The steel samples were dried and weighed. X-ray diffraction (XRD), scanning electron microscopy (SEM) and electron dispersive spectroscopy (EDS) analyses were performed before the ASTM G1²⁹ procedure was followed to remove the corrosion products and determine the corrosion rate by weight loss. Surface profile analysis was then performed to investigate the extent of localized corrosion.

Flow loop experimental results

Pictures of the weight loss samples taken immediately after the end of the test and after removal of the corrosion product layer are shown in Figure 4 (Test 1) and Figure 5 (Test 2). SEM/EDX analysis is also presented. The morphology of the corrosion product layer could be quite varied from very small crystallites seen in Test 1 (at low water condensation rate) to a more amorphous layer seen in Test 2 (at higher water condensation rate). The presence of FeS was identified in both tests as expected, although no phase identification could be performed.

Once the corrosion product layer was removed, the steel surface looked fairly uniform with only sparse traces of localized corrosion with isolated pits ranging from 80 to 130 μm in depth. The maximum pitting rate is then calculated at 1.3 mm/year for Test 1 and 2.7 mm/year for Test 2. However, it should be mentioned that the percentage of the coupon surface affected by localized corrosion was very small in both tests. The pits could not be found with simple visual inspection and required the use of a surface profilometer to be identified.



©2012 by NACE International. Requests for permission to publish this manuscript in any form, in part or in whole, must be in writing to NACE International, Publications Division, 1440 South Creek Drive, Houston, Texas 77084. The material presented and the views expressed in this paper are solely those of the Flow Loop Test and are not necessarily endorsed by the Association.

Figure 4. Analysis of the corrosion product layer
Flow Loop Test 1, top of the line test duration 19 days

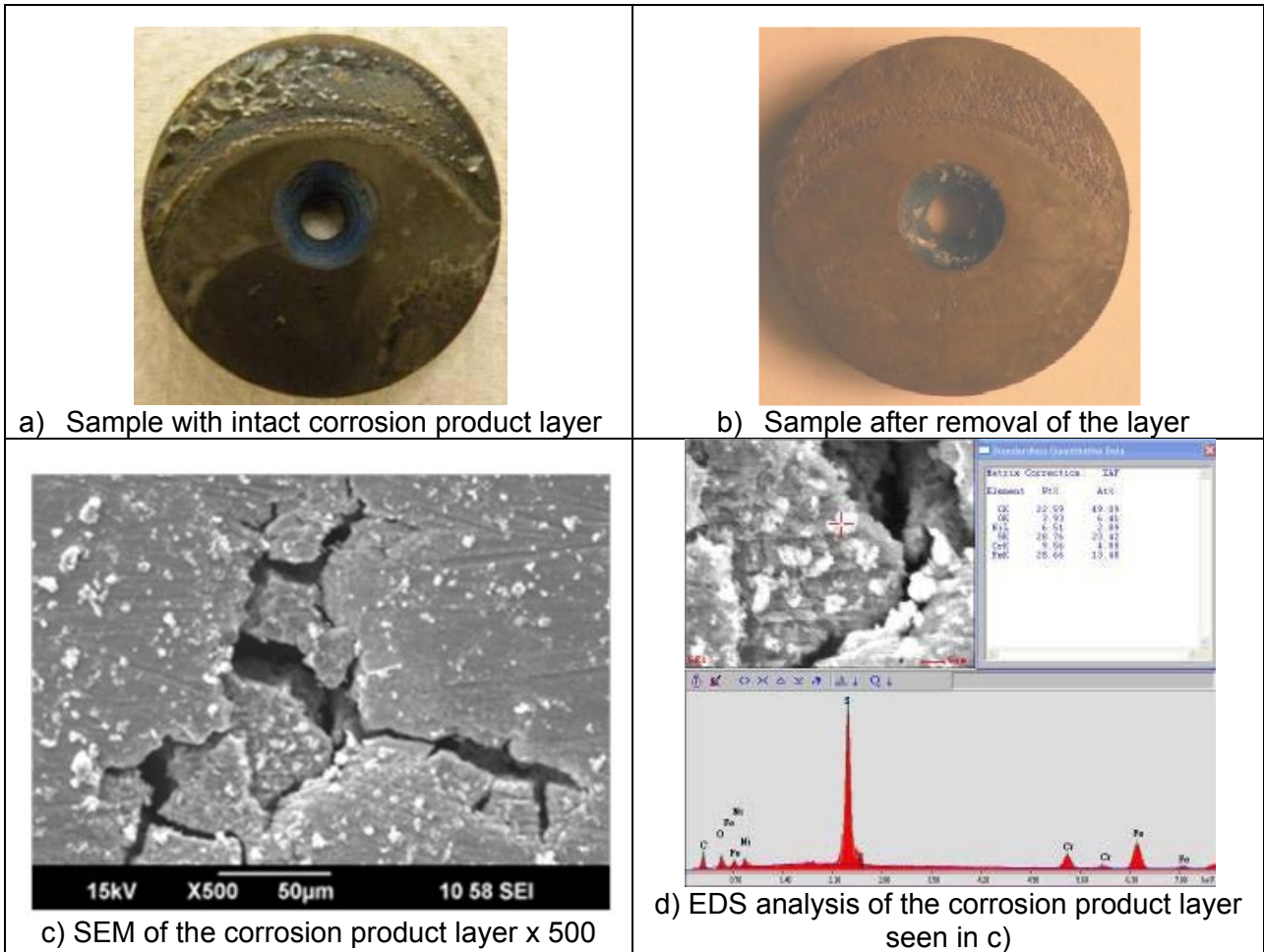


Figure 5: Analysis of the corrosion product layer
Flow loop Test 2 - top of the line - duration: 22 days.

Figure 6 shows the general corrosion rate results obtained in the two large scale flow loop tests. The number above each data point represents the number of weight loss samples used to calculate the average TLC rate and the error bar corresponds to the maximum and minimum TLC rates measured.

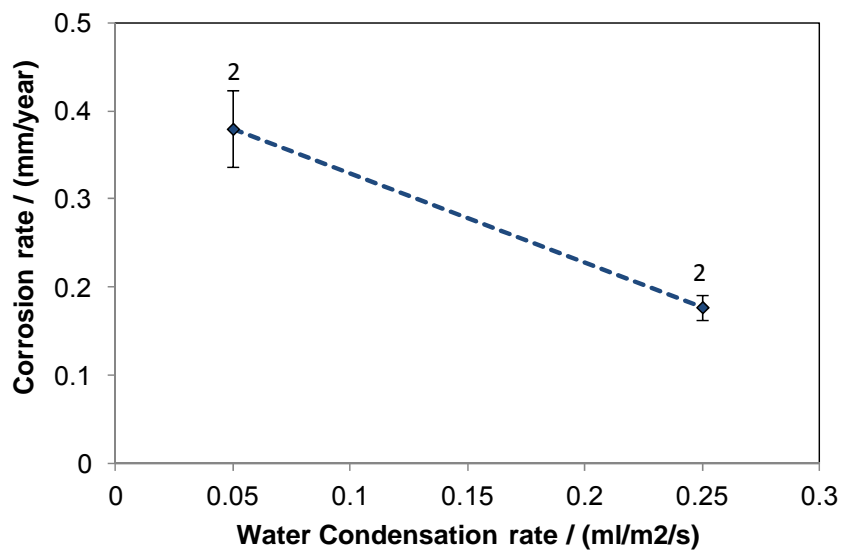


Figure 6: TLC rate comparison between results from Test 1 (undissociated HAc= 250 ppm

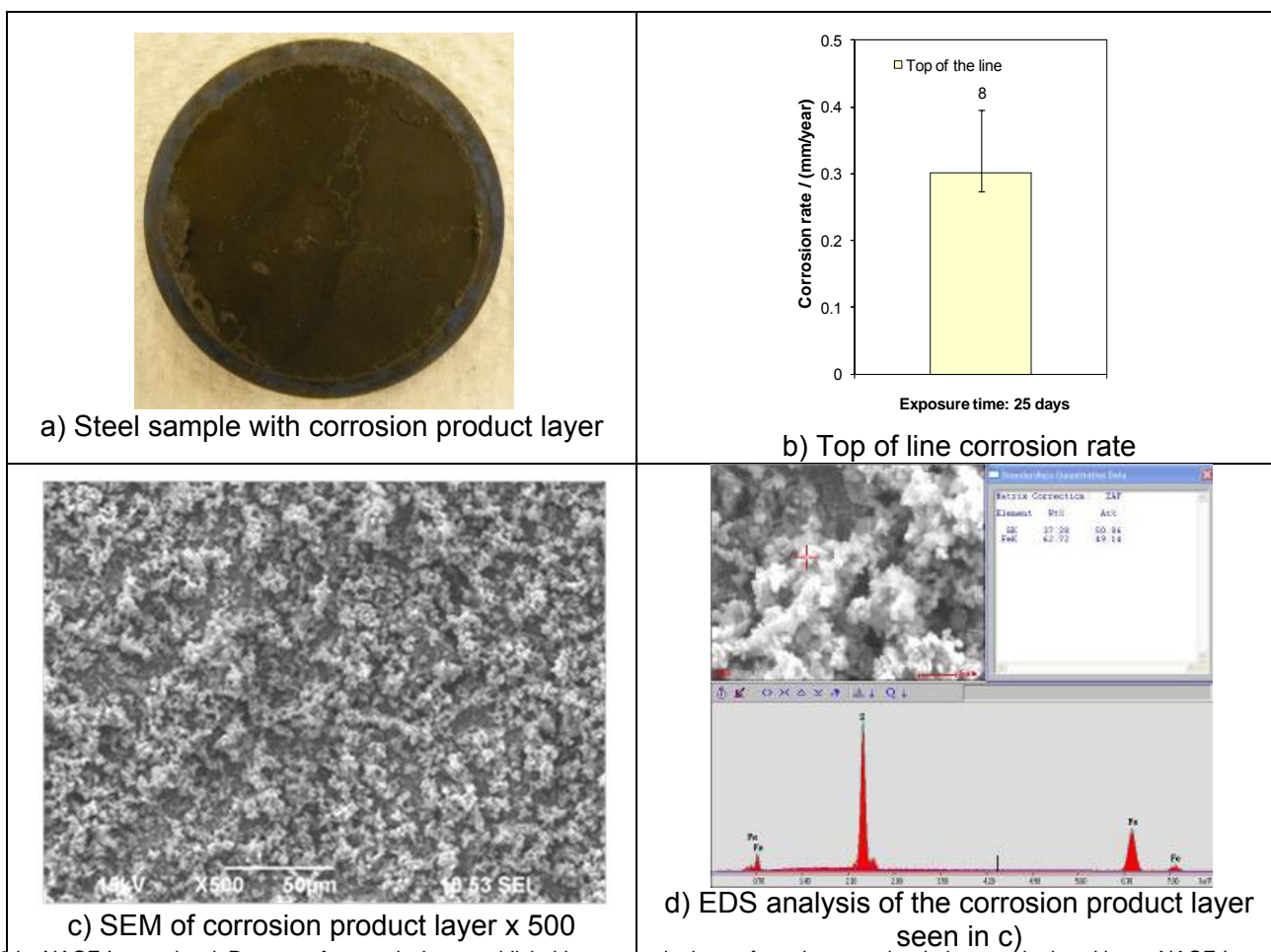
In Test 2, the concentration of undissociated acetic acid is slightly higher than in Test 1 (upon the request for the sponsor of the study). The results seem to show that the water condensation rate has little to no effect on the general corrosion rate. This is contrary to the sweet CO₂ dominated TLC where the condensation rate has a definite influence on the corrosion rate. Although any explanation at this stage is tentative, it can be inferred that since FeS does not need significant bulk supersaturation to form on the steel surface (as opposed to FeCO₃) the amount of water condensing should not matter as much as it does in CO₂ dominated TLC. This does not mean, however, that the condensation has no effect. The presence of water condensing on the steel sample is still essential for the corrosion reactions to happen.

Autoclave experimental results

This section presents in detail the results obtained with the 20L autoclave. The objective of Test 3 was to build a link between the large flow loop and the autoclave tests, as similar conditions were used. Tests 4 - 7 focused on simulating the Karan field conditions more closely.

Test 3: Comparison between flow loop and autoclave results

Although the conditions are not exactly identical (T_{gas} : 40°C instead of 55°C for the flow loop tests), these experiments are similar enough to make a comparison. The results of the autoclave test are shown in Figure 7. The TLC rate shows good repeatability and does agree rather well within the flow loop results (0.3 mm/year for the autoclave compared to 0.2-0.4 mm/year for the flow loop over a 3 week period) giving encouraging evidence that autoclave tests should be able to produce reliable TLC data. The corrosion product analysis showed the presence of a porous superficial layer identified as an iron sulfide (most likely mackinawite although no XRD analysis was performed). The sample was uniformly corroded and no trace of localized corrosion could be found during the surface profile analysis (not shown here).



©2012 by NACE International. Requests for permission to publish this manuscript in any form, in part or in whole, must be in writing to NACE International, Publications Division, 1440 South Creek Drive, Houston, Texas 77084. The material presented and the views expressed in this paper are solely those of the Autoclave Test 3 - top of the line exposure time 25 days.

Tests 4 - 7: Influence of high partial pressure of H₂S on TLC

Photographs of the weight loss samples taken immediately after the end of the test are shown in Figure 8. The steel samples have very similar appearance with a grey layer covering the entire surface. Rounded markings are visible and are indications of the presence of droplets of condensed water, typically 10 to 12 mm diameter, on the surface of the steel samples. No clear indication of breakdowns in the corrosion product layer could be observed.

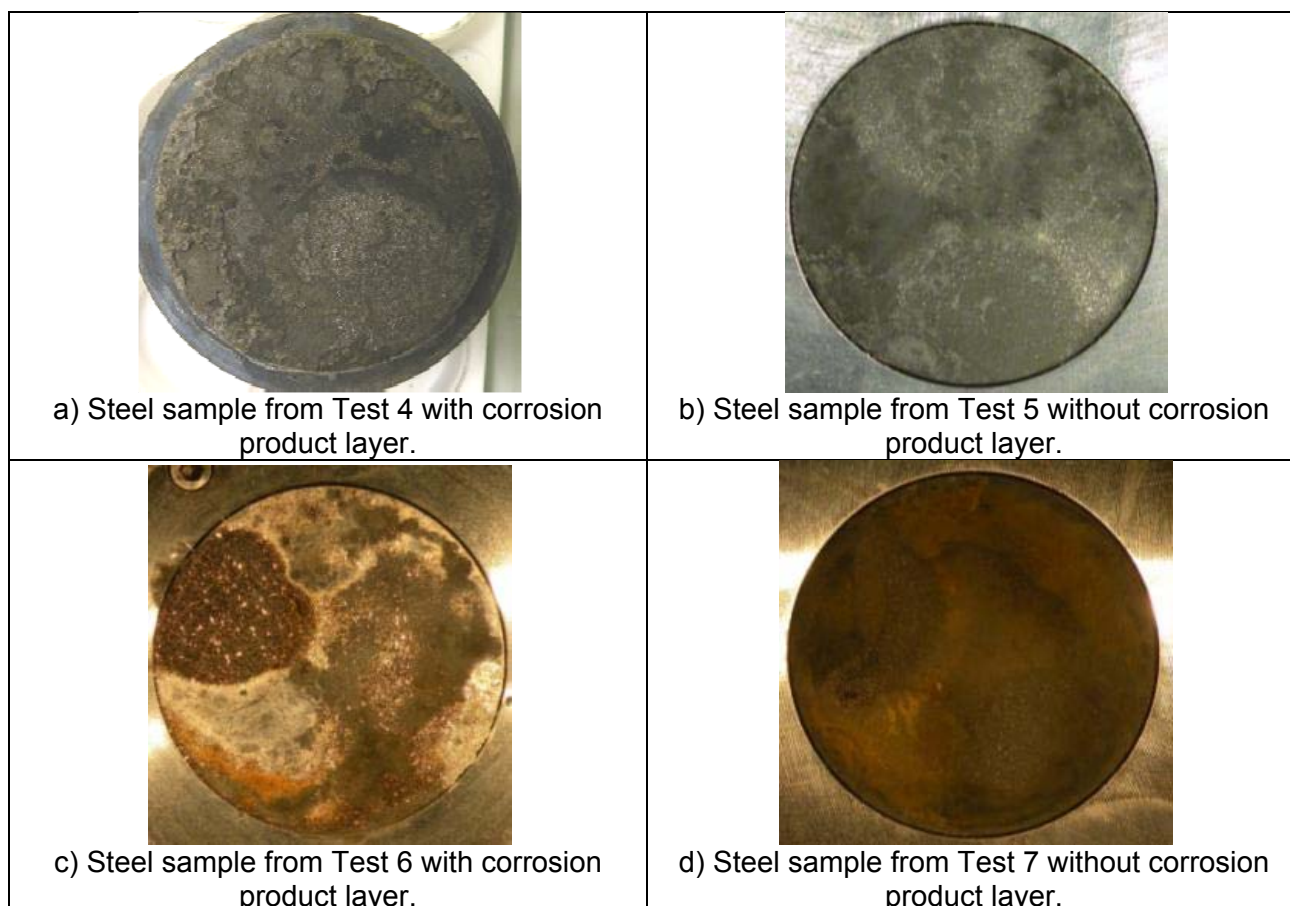


Figure 8: WL coupons before (left) and after (right) the removal of the corrosion product Autoclave Tests 4, 5, 6, 7- top of the line - exposure time: 21 days.

The SEM/EDX analysis of the corrosion product layer is shown in Figure 11 together with corresponding XRD analysis of the corrosion product layer. Unusual features could be observed by SEM, all apparently being forms of FeS as suggested by using the EDX elemental analysis. The variety of the morphologies observed infers that potentially different phases of FeS formed on the steel surface.

For Test 4 (1.2 bars of H₂S, T_{gas}: 45°C), XRD analysis identified the corrosion product layer as comprising of mackinawite and cubic FeS. Similar to mackinawite, cubic FeS is a by-product of sour corrosion of mild steel and is reported to form very well defined crystals at pH between 4 and 5 and at temperature between 35 and 60°C.²⁶ Cubic FeS converts to mackinawite with time and is not believed to be a stable phase of FeS.

Test 5 and test 7 were performed at a higher condensation rate (0.12 and 0.14 mL/m²/s), at two different H₂S partial pressures (2 and 4.3 bars, respectively) and at higher temperature (T_{gas}: 55°C). The XRD/SEM analyses performed on the coupon surfaces are quite similar as reported above for Test 4. The presence of mackinawite was identified in both cases together with very small amounts of cubic FeS in Test 5 (pH₂S: 1.99 bars).

For Test 6 (low water condensation rate, T_{gas}: 55°C, pH₂S: 4.3 bars), the XRD analysis performed on the coupon surface identified the presence of mackinawite and traces of troilite (stoichiometric

For comparison, standard diffraction line intensities for troilite, mackinawite and cubic FeS are shown in Figure 9.

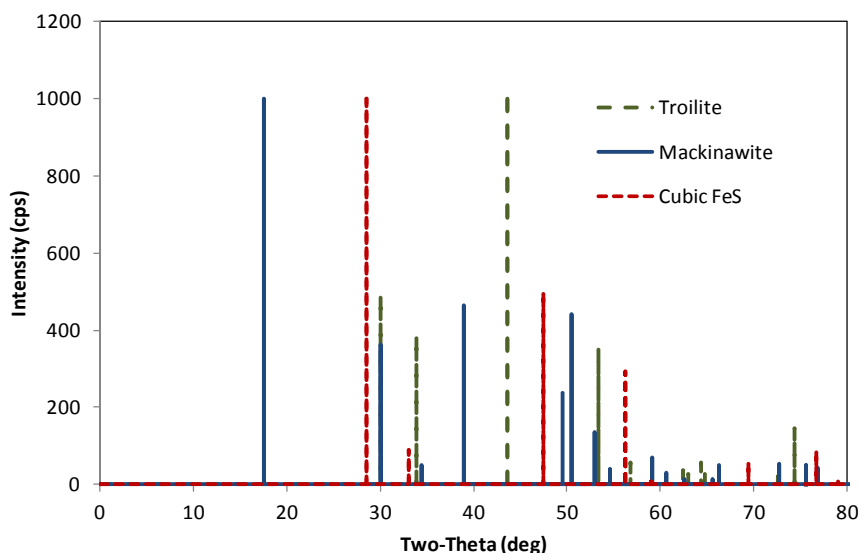


Figure 9: XRD analysis – standard pics for troilite, mackinawite and cubic FeS
Autoclave Tests 4, 5, 6, 7- top of the line - exposure time: 21 days.

The work of Smith^{30, 31, 32} is helpful in providing explanations for the occurrence of different iron sulfide corrosion products. At relatively low temperature, mackinawite is favoured in short term exposures as the kinetics of mackinawite formation are faster than any other FeS species. The formation of cubic FeS (metastable phase transitioning to pyrrhotite or mackinawite), troilite (stoichiometric pyrrhotite) or pyrrhotite is more complex. Figure 10 is the representation of the domain of stability of each stable FeS phase.

In the experiment performed, the condensed water is obviously free of salt and should have a rather low pH (between 3.5 and 4.5). These conditions would favour the subsequent formation of cubic FeS. However, this product degrades over time to mackinawite or pyrrhotite and is never encountered in the field. Troilite has been observed in top of the line scenarios before²⁸ with characteristic needle-shaped crystals. Troilite is a stoichiometric form of pyrrhotite. At the higher condensation rate tests (Test 5 and 7), the temperature of the sample was measured to be around 20-25°C which could explain why only mackinawite was detected. Tests 6 and 7 were performed at much lower condensation rates and the steel temperature was consequently higher (38°C for test 4 and 50°C for test 6). This should tend to favour the formation of the kinetically slower-to-form troilite or pyrrhotite, or even cubic FeS. In addition, traces of troilite were found in test 6 for which the partial pressure of H₂S was the highest (4.3 bars).

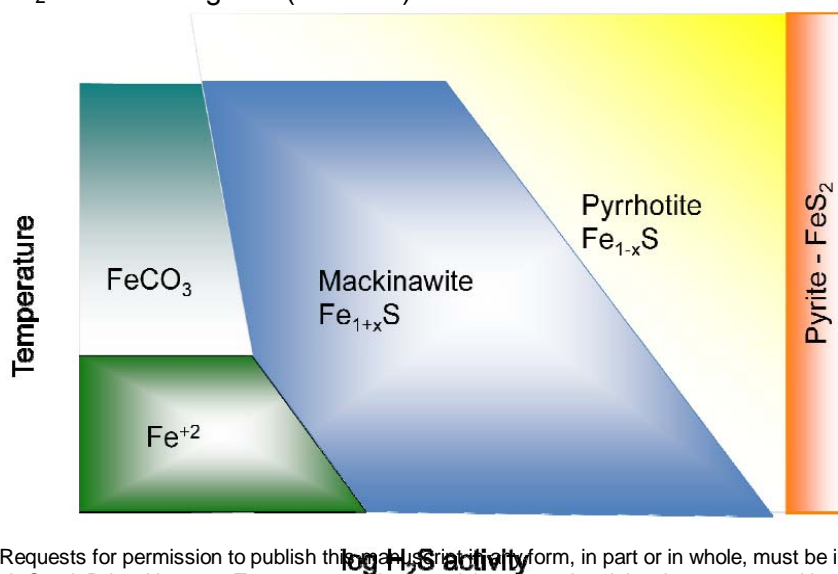
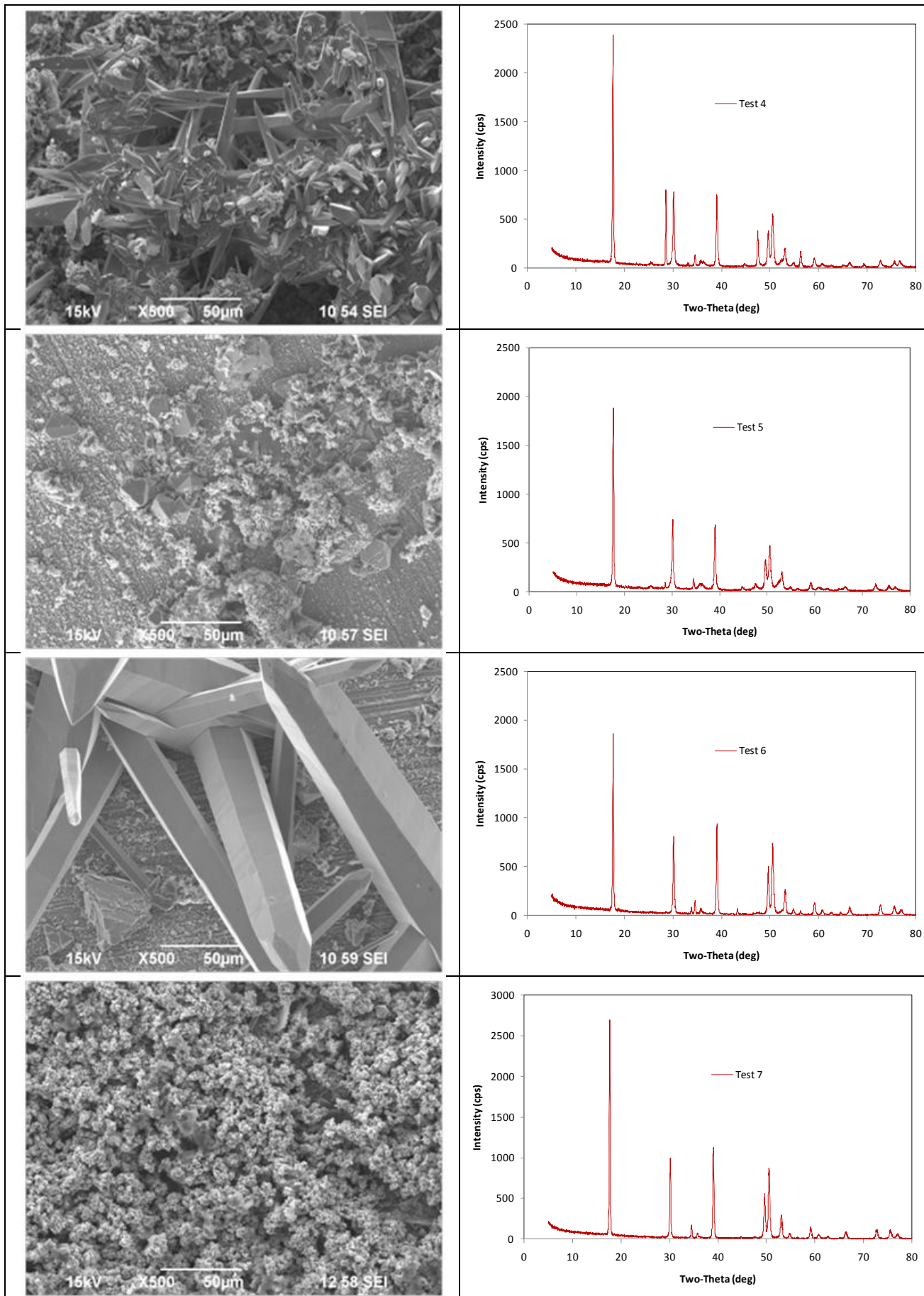


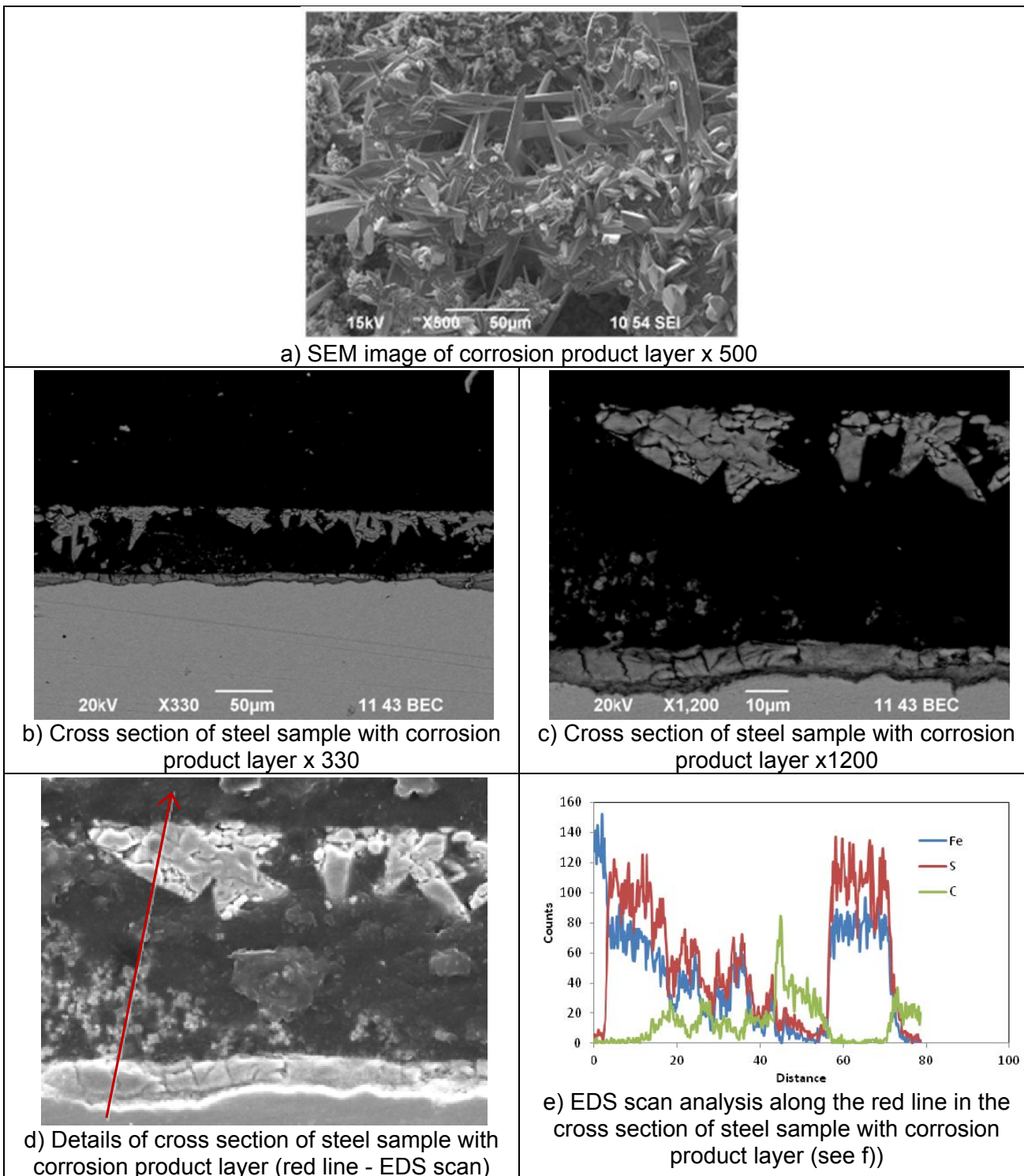
Figure 10: Stability of Fe-S products with regard to temperature and H₂S activity



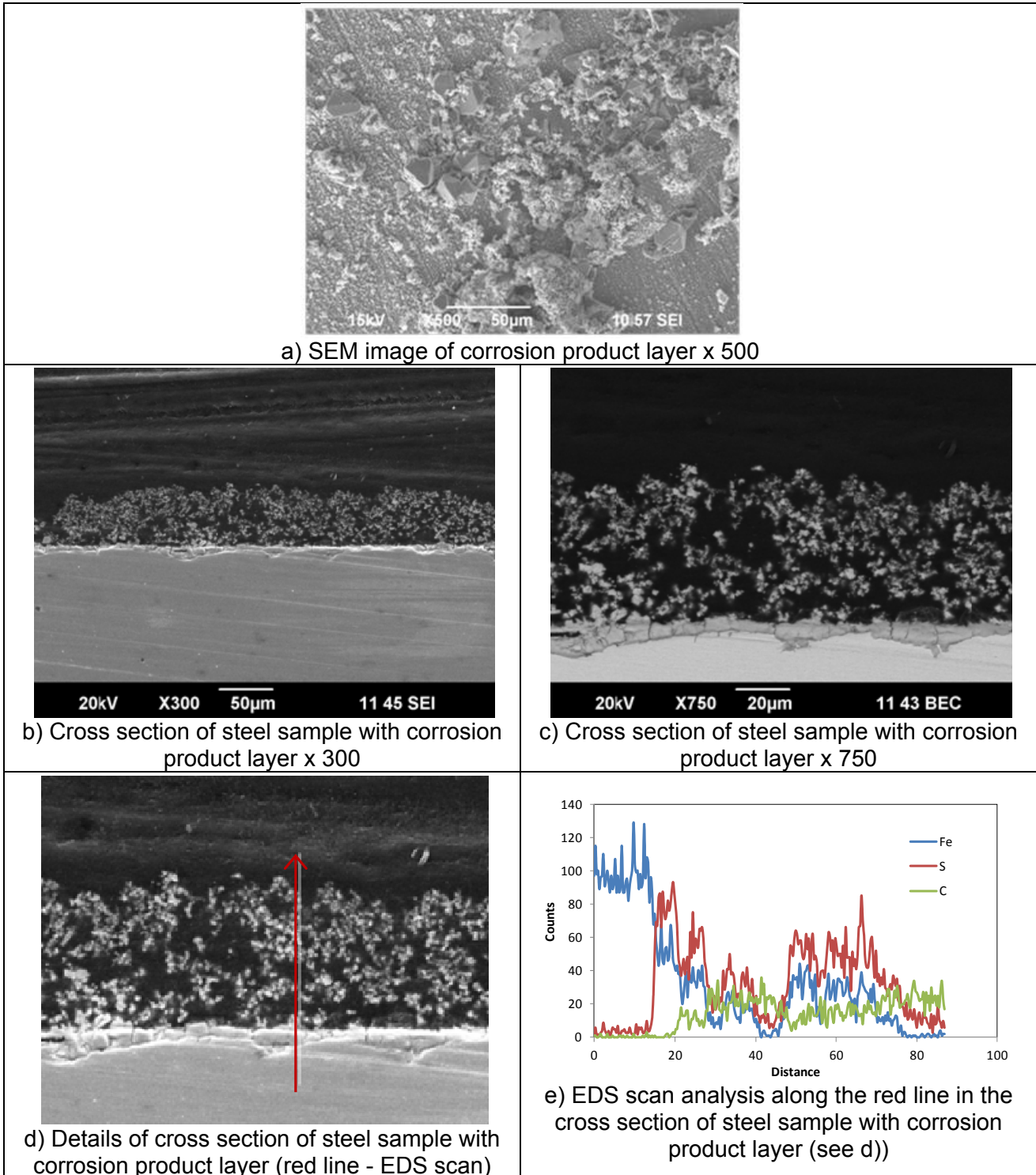
©2012 by NACE International. Reproduction of this document is prohibited without the express written permission of NACE International, Publications Division, 1440 South Creek Drive, Houston, Texas 77084. The material presented and the views expressed in this paper are solely those of the author(s) and are not necessarily endorsed by the Association.

Figure 1. SEM and XRD analysis of the corrosion product layer
Autoclave Test 4, 5, 6, 7- top of the line - exposure time: 21 days.

Cross section analysis was also performed and the results are presented in Figure 12 to Figure 15. For test 4, it can be seen that the very dense and adherent FeS layer which forms on the metal surface has a thickness between 10 and 20 μm while it is calculated that the steel lost on average 13.7 μm due to corrosion. There is therefore a close match between the thickness of the lower portion of the adherent layer and the steel thickness loss. However, different locations of the cross section show the presence of features above this dense layer although no clear difference in chemical composition was found between the two. This outer layer of FeS is not as well attached to and probably corresponds to the larger features observed in other SEM images. Nevertheless, the overall roughness of the steel surface does indicate that the corrosion attack was uniform.



For test 5, the FeS layer is also composed of two parts: a dense and adherent layer covering the steel surface with a thickness on average of just under 7 μm ; and a second very porous layer on top of the previous one, with an average thickness of about 40 μm . By comparison, the steel thickness loss due to corrosion is 4.5 μm which corresponds roughly to the thickness of the first layer. The porosity of the second layer can be inferred by observing the SEM images. Since the second outer layer is much thicker than the calculated “wall thickness loss”, it has most likely have formed through a precipitation process. The EDS elemental analysis shows no significant chemical composition difference between the two types of layers, both identified as FeS. In addition, no localized corrosion could be observed on the bare steel surface once the layer was removed.



©2012 by NACE International. This document is for personal use only. All rights reserved. No part of this document may be reproduced, stored in a retrieval system, or transmitted, in any form or by any means, electronic, mechanical, photocopying, recording, or by any information storage and retrieval system, without the prior written permission of NACE International, Publications Division, 1440 South Creek Drive, Houston, Texas 77084. The material presented and the views expressed in this paper are solely those of the author(s) and are not necessarily endorsed by the Association.

As observed in the two previous tests, the corrosion product layer for Test 6 again seems to comprise of two distinct layers on top of each other. A first dense and seemingly adherent layer covers the steel surface with a thickness around 10 μm (which is significantly more than the average 4 μm wall loss). On top of this first layer, larger features corresponding to the “troilite needles” could be found which corresponds to the crystals observed in the SEM images. Both layers have similar chemical composition. Once again, no localized corrosion could be found on the bare metal surface.

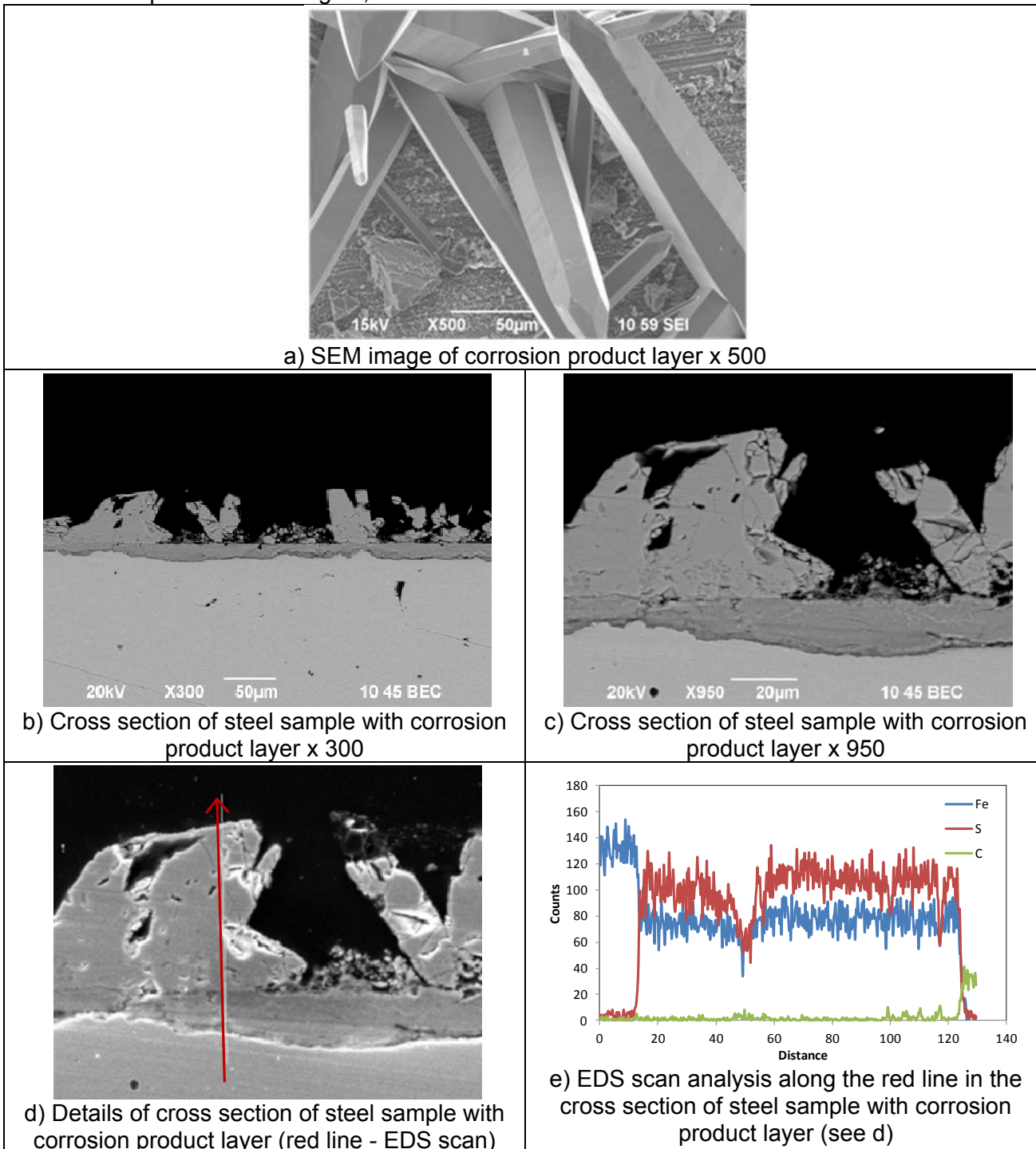


Figure 14: Cross section analysis of steel sample with corrosion product layer; Autoclave Test 6 - top of the line – duration 21 days

Finally for test 7, the corrosion product layer presents the same characteristics as were observed at higher condensation rates in Test 5. Thick and very porous layer covers a more dense and adherent inner film. The porous layer is about 25-30 μm thick while the dense layer is on average only 10 μm thick. By comparison, the wall loss by corrosion is 75 μm . The small crystals trapped in the epoxy matrix seen in the cross sectional images correspond to those observed in the SEM images of the

corrosion product layer surface. Once again, there were no chemical composition differences between the two layers and the corrosion attack was uniform. Although no surface profile analysis is shown in this paper, the metal surface of all the samples was always uniformly corroded and no trace of localized corrosion could be found.

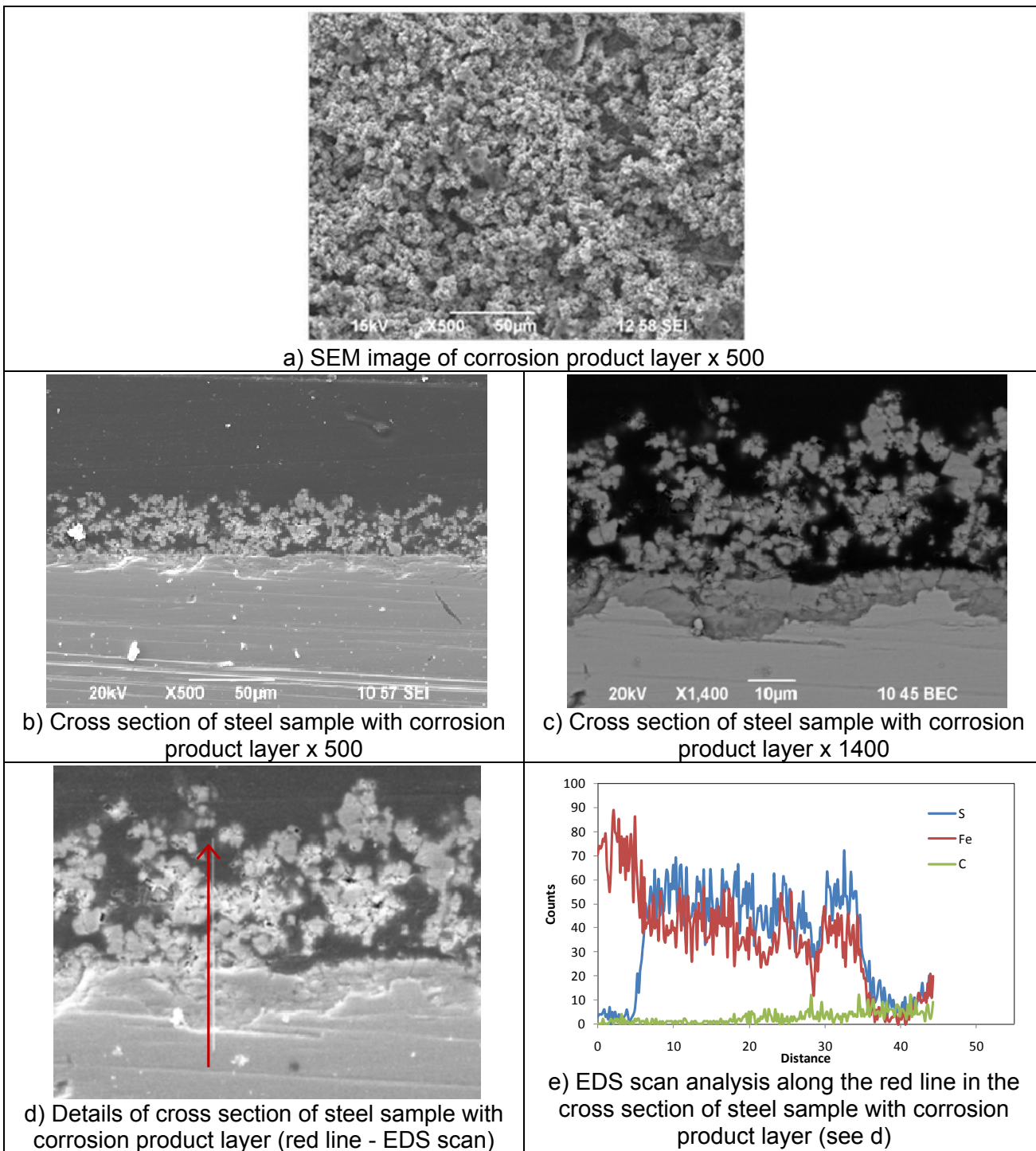
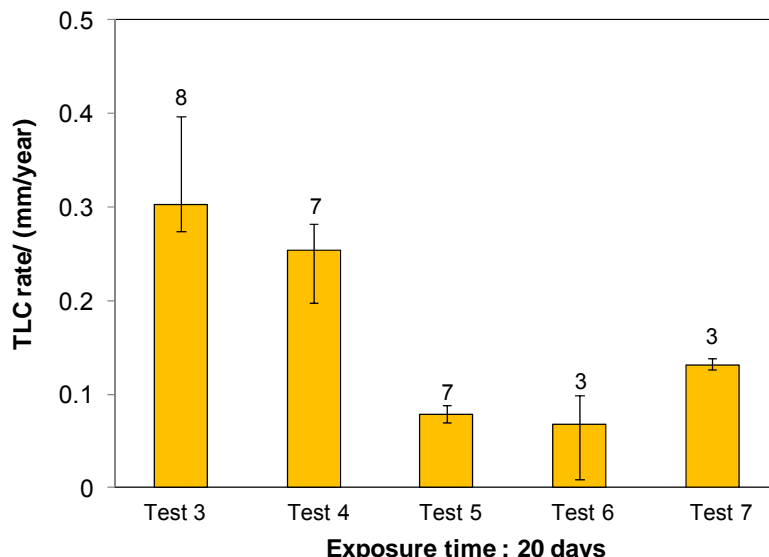


Figure 15: Cross section analysis - Autoclave Test#7 (21 days) - Top of the line

Considering the differences in the kinetics of formation of mackinawite vs cubic FeS or troilite/pyrrhoite, Smith³⁰ proposed a two step mechanism involving the rapid formation of a thin mackinawite layer on the metal surface “overlain” by potentially different phases of iron sulfide. This “two steps” mechanism seems to be validated by the analysis of the cross section performed in this study. The growth rate of the first layer seems to be directly related to the corrosion rate as its thickness often corresponds to the uniform metal loss. The density of the second phase depends more on the actual test conditions than on the kinetics of corrosion product formation. Low

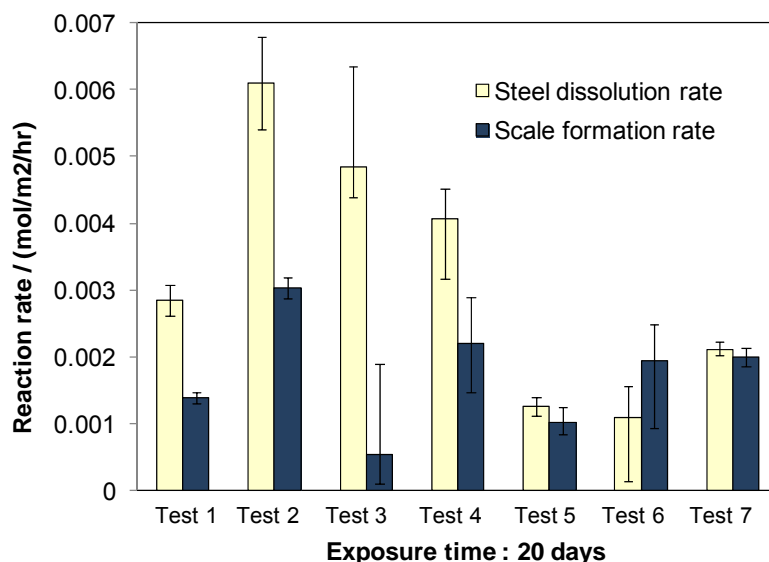
temperature (linked to higher condensation rate) seems to favour the formation of a very porous mackinawite. At higher temperature (45 – 50°C), cubic FeS crystals can nucleate more rapidly. Higher temperature and higher H₂S partial pressure lead to the formation of troilite and probably pyrrhotite. The corrosion rate for each of the autoclave tests are shown in Figure 16 together with a summary of the most influential parameters (pH₂S, gas temperature, steel surface temperature, water condensation rate). It is not very easy to compare the test results as more than one parameter changed between experiments and an effort to isolate the influence of each parameter is made in the next section.



	Test 3	Test 4	Test 5	Test 6	Test 7
pH ₂ S / (bar):	0.11	1.99	1.24	4.29	4.29
WCR / (ml/m ² /s):	0.14	0.02	0.12	0.02	0.14
T _{gas} / (°C):	40	45	55	55	55
T _{steel surface} / (°C):	17	38.1	21.4	50	24.4
pCO ₂ / (bar)	0.41	8.13	9.4	9.9	9.9

Figure 16: Autoclave tests - corrosion rate analysis
- top of the line - exposure time: 21 days.

Figure 17 presents a comparison between the time-averaged flux of Fe²⁺ leaving the steel and the time-averaged flux of Fe²⁺ consumed for the FeS scale formation. Using the same unit of mol_{Fe2+}/m²/s, the steel dissolution rate (corrosion rate) and the scale formation rate (formation rate of FeS) can be compared.



	Test 1	Test 2	Test 3	Test 4	Test 5	Test 6	Test 7
pH ₂ S / (bar):	0.1	0.1	0.11	1.99	1.24	4.29	4.29
WCR / (ml/m ² /s):	0.25	0.05	0.14	0.02	0.12	0.02	0.14
T _{gas} / (°C):	55	55	40	45	55	55	55
T _{steel surface} / (°C):	~25	~50	17	38.1	21.4	50	24.4
pCO ₂ / (bar)	0.41	8.13	9.4	9.9	9.9	9.9	9.9

Figure 17: Comparison between scale formation rate and steel dissolution rate

In all cases, the layer is assumed to be entirely made of mackinawite. This graph helps evaluating how much of the iron dissolved by corrosion ends up being used in the layer formation process. In this TLC scenario, the Fe^{2+} ions present in the condensed water can only come from the corrosion process happening *in situ* as there is no bulk solution like there is at the bottom of the line. Consequently, the scale formation rate should always be lower or equal to the steel dissolution rate and that is the case in most of the experiments performed herein. Often, about half of all the Fe^{2+} ions released through corrosion are used for the FeS layer formation although there is a scatter in the results. The results obtained through Test 6 show, however, the opposite behaviour with a scale formation rate being higher than the steel dissolution rate. This discrepancy is not explained to this date and could be due to errors related to trapping of water within formed corrosion product layers, iron sulfide oxidation by atmospheric O_2 during sample recovery or through balance error.

Discussion

The following graphs (Figure 18 to Figure 22) plot the average corrosion rate *versus* what are considered to be key parameters. However, it should be understood that many conditions changed between the tests (temperature, pH_2S and condensation rate) and that the comparison cannot be made directly.

The effect of the condensation rate is analyzed first as in CO_2 dominated TLC, condensation has a primary influence. In that case low condensation rates lead to high pH and high super-saturation with respect to FeCO_3 inside the droplets. A protective layer forms and the corrosion remains low. If the condensation rate is higher (critical value of $0.25 \text{ ml/m}^2/\text{s}$ or $0.025 \text{ ml/m}^2/\text{s}$ have been proposed), sufficient saturation levels to ensure FeCO_3 stability cannot be achieved and high general or localized corrosion rates are experienced. In sour systems, the FeS layer is fairly insoluble in water and FeS formation occurs almost instantaneously at the metal surface. In these conditions, it is believed that the pH in the condensed water remains always quite low and the effect of the condensation rate is minimized²⁷. This is what is seen in Figure 18, where the influence of the condensation is not present. This said, if test 6 and 7 are directly compared, a tenfold increase in the condensation rate (from 0.02 to $0.14 \text{ ml/m}^2/\text{s}$) leads to a doubling of the corrosion rate (from 0.07 to 0.12 mm/year). However, this effect is believed to be overcome by other parameters such as the temperature.

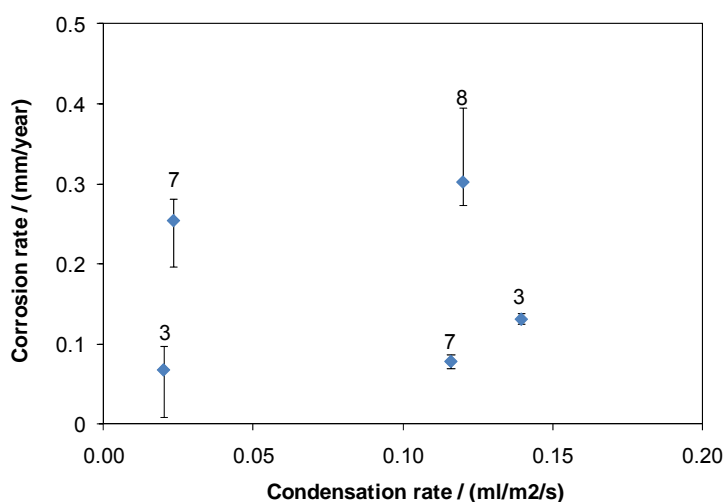


Figure 18: Influence of the water condensation rate on TLC.

Looking at the effect of the partial pressure of H_2S or the $\text{CO}_2/\text{H}_2\text{S}$ ratio (Figure 19 and Figure 20), no correlation with corrosion behaviour is apparent. On one hand higher partial pressure of H_2S should lead to a more aggressive environment while on the other corrosion attack produces more

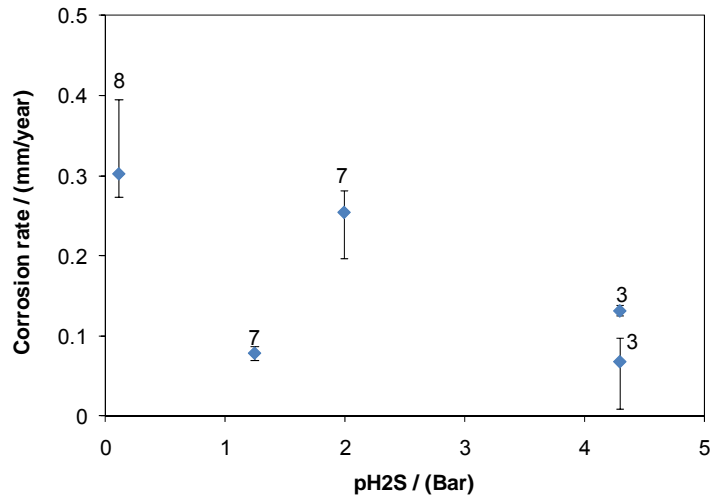


Figure 19: Influence of the partial pressure of H₂S on TLC.

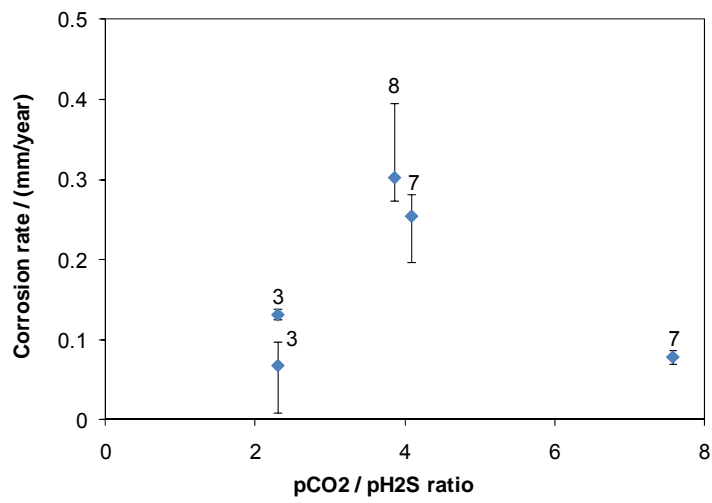


Figure 20: Influence of the partial pressure CO₂/H₂S ratio on TLC.

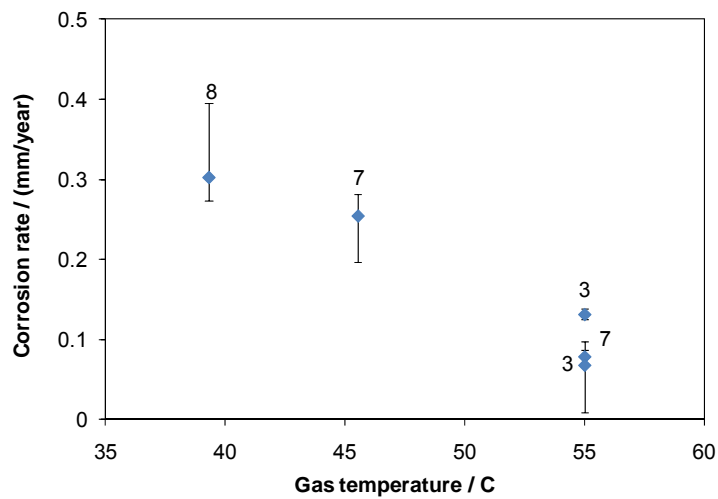


Figure 21: Influence of the gas temperature on TLC.

Figure 21 shows the influence of the gas temperature and there seems to be a correlation with the corrosion rate. As it has been previously reported in the literature¹⁸, higher corrosion rates are reported at lower temperature. In the experiments performed for this study, the highest corrosion rates were reported at lowest temperature (below 45°C). However, the corrosion reaction including layer formation should be controlled by the temperature at which it occurs, *i.e.*, the steel temperature instead of the gas temperature, which can be quite different. Figure 22 shows the corrosion rate plotted *versus* the steel surface temperature which is calculated based on an in-house condensation rate model. No correlation could be seen here which is unexpected. One can question the validity of the temperature predictions, assuming they are not accurate, which is unlikely since the accuracy has been validated against controlled laboratory environments. The other possibility is that the overall process is controlled by the liquid/vapor equilibrium reactions which depend more on the gas temperature.

Finally, one can look back for a potential influence of the FeS layer composition or phase. Considering the results available from the XRD analysis (Test 4 to 7), the highest corrosion rate was measured when a mixture of cubic FeS and mackinawite was detected on the steel surface. Pure mackinawite seems to lead preferably to general attack and to a lower corrosion rate. Further work is definitively needed in this area.

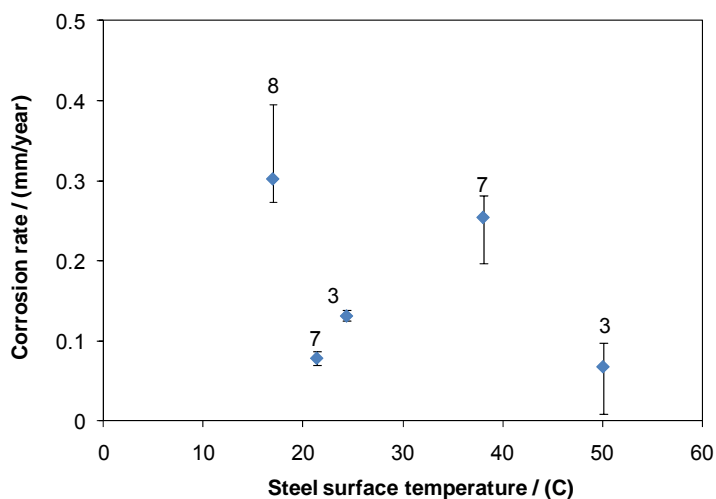


Figure 22: Influence of the steel surface temperature on TLC.

CONCLUSIONS

- The 20L autoclave seems to produce reliable data as compared to the large scale (2000L) multiphase flow loop tests. It also enabled a more representative simulation of the field conditions with regard to the high H₂S partial pressure.
- The experiments conducted here in sour conditions resulted in relatively low average corrosion rates under water condensing conditions (below 0.5 mm/year) in both flow loop and autoclave tests.
- One instance of localized corrosion was observed in a flow loop test (pitting rate of 2.7 mm/year after 21 days of testing).
- The corrosion attack seems to be controlled mainly by the gas temperature (lower temperature leading to higher corrosion rate). The protective properties of the FeS formed seem to play a key role. Mackinawite, cubic FeS and troilite were identified by XRD in the corrosion product layer. The condensation rate, partial pressure of H₂S or H₂S/CO₂ ratio did not seem to have a clear influence on the corrosion rate.

ACKNOWLEDGMENTS

The authors would like to acknowledge the technical guidance and financial support provided by Saudi Aramco and by the other sponsoring companies of the Top of the Line Corrosion Joint Industry Project at Ohio University: Total, BP, ConocoPhillips, Chevron, Occidental Oil Company, ENI, and PTTEP.

REFERENCES

1. Paillassa R., Dieumegard M., Estevoyer M., "Corrosion control in the gathering system at Lacq sour gas field", 2nd Intl. Congress of Metallic Corrosion, NACE, pp 410-417, New York, 1963.
2. Gunaltun Y.M., Supriyataman D., Jumakludin A., "Top of the line corrosion in multiphase gas line. A case history", Corrosion 99, paper 36 (Houston, TX: NACE International, 1999).
3. Thammachart M., Gunaltun Y., Punpruk S., "The use of inspection results for the evaluation of batch treatment efficiency and the remaining life of the pipelines subjected to top of line corrosion", Corrosion 08, paper 8471 (New Orleans, LA: NACE International 2008).
4. Gunaltun Y., Larrey D., "Correlation of cases of top of the line corrosion with calculated water condensation rates", Corrosion 00, paper 71 (Houston, TX: NACE International, 2000).
5. Ho-Chung-Qui D.F., Williamson A.I., Eng P., "Corrosion experiences and inhibition practices in wet sour gathering systems", Corrosion 87, Paper 46 (San Francisco, CA: NACE International, 1987).
6. Bich N.N., Szklarz K.E., "Crossfield Corrosion Experience", Corrosion 88, Paper 196 (Saint Louis, MI: NACE International, 1988).
7. Edwards M., Cramer B., "Top of the line corrosion –Diagnostic, root cause analysis and treatment", Corrosion 00, Paper 72 (Houston, TX: NACE International, 2000).
8. Martin R.L., "Control of Top-of-line Corrosion in Sour Gas Gathering Pipeline with Corrosion Inhibitors", Corrosion 09, Paper 9288 (Atlanta, GA: NACE International, 2009).
9. Joosten M., Owens D., Hobbins A., Sun H., Achour M., Lanktree D., "Top-of-line corrosion – A field failure", EuroCorr 10, Paper 9524, Moscow, Russia.
10. Singer M., Nestic S., Gunaltun Y., "Top of the line corrosion in presence of acetic acid and carbon dioxide", Corrosion 04, paper 4377 (Houston, TX: NACE International, 2004).
11. Mendez C., Singer M., Camacho C., Hernandez S., Nestic S., "Effect of acetic acid, pH and MEG on the CO₂ top of the line corrosion", Corrosion 05, paper 5278 (Houston, TX: NACE International, 2005).
12. Andersen T., Halvorsen A.M.K., A. Valle A., Kojen G., "The influence of condensation rate and acetic acid concentration on TOL corrosion in multiphase pipelines", Corrosion 07, paper 7312 (Nashville TN, NACE International 2007).
13. Nyborg R., Dugstad A., "Top of the line corrosion and water condensation rates in wet gas pipelines", Corrosion 07, paper 7555 (Nashville TN, NACE International 2007).
14. Hinkson D., Singer M., Zhang Z., Nestic S., "A study of the chemical composition and corrosivity of the condensate in top of the line corrosion", Corrosion 08, paper 8466 (New Orleans, LA: NACE International 2008).
15. Singer M., Nestic S., Hinkson D., Zhang Z., Wang H., "CO₂ top of the line corrosion in presence of acetic acid - A parametric study", Corrosion 09, paper 9292 (Atlanta, GA: NACE International, 2009).
16. Camacho A., Singer M., Brown B., Nestic S., "Top of the Line Corrosion in H₂S/CO₂ Environments", Corrosion 08, paper 8470 (New Orleans, LA: NACE International 2008).

17. Nyborg R., Dugstad A., Martin T., "Top of Line Corrosion with High CO₂ and Traces of H₂S", Corrosion 09, Paper 9283 (Atlanta, GA: NACE International, 2009).
18. Pugh D.V. et al, "Top-of-Line Corrosion Mechanism for Sour Wet Gas Pipelines", Corrosion 09, Paper 9285 (Atlanta, GA: NACE International, 2009).
19. Bonis, M, "Form sweet to sour TLC: what's different?", Second International TLC Conference, Bangkok, 2009.
20. Valdes A., Case R., Ramirez M., Ruiz A., "The effect of small amounts of H₂S on CO₂ corrosion of carbon steel," Corrosion 98, paper 22 (Houston, TX: NACE International, 1998).
21. Kvarekval J., "The influence of small amounts of H₂S on CO₂ corrosion of iron and carbon steel," Eurocorr 97, Trondheim, Norway.
22. Brown B., Lee K.L., Nestic S., "Corrosion in multiphase flow containing small amounts of H₂S", Corrosion 03, paper 3341 (Houston, TX: NACE International, 2003).
23. Brown B., Reddy Parakala S., Nestic S., "CO₂ corrosion in presence of trace amounts of H₂S", Corrosion 03, paper 4736 (Houston, TX: NACE International, 2004).
24. Smith S., Joosten M., "Corrosion of carbon steel by H₂S in CO₂ containing environments", Corrosion 06, paper 6115 (Houston, TX: NACE International, 2006).
25. Singer M., Brown B., Camacho A., Nestic S., "Combined effect of CO₂, H₂S and acetic acid on bottom of the line corrosion", Corrosion/07, paper# 7661 (Nashville TN, NACE International 2007).
26. Murowchick, J.B., Barnes H.L., "Formation of cubic FeS", *American Mineralogist*, Vol.71, pp. 1243-1246, 1986.
27. Joosten M., Oweens D., Hobbins A., Sun H., Achour M., Lanktree D., "Top-of-Line Corrosion – A Field Failure", paper# 9524 (Russia, EuroCorr 2010).
28. Singer M., Camacho A., Brown B., and Nestic S., "Sour Top-of-the-Line Corrosion in the Presence of Acetic Acid", *Corrosion*, 67, 085003 (2011).
29. ASTM G1, "Standard Practice for Preparing, Cleaning, and Evaluating Corrosion Test Specimens," in *ASTM Standard*, vol. 03.02, West Conshohocken, PA: ASTM, 2003.
30. Smith S., Brown B., Sun W., "Corrosion at higher H₂S concentrations and moderate temperatures", Corrosion/11, paper# 11081 (Houston, TX: NACE International, 2011).
31. Smith S., Wright E.J., "Prediction of minimum H₂S Levels required for slightly sour corrosion", Corrosion 94, paper# 11, (Houston, TX: NACE International, 1994).
32. Smith S., "A proposed mechanism for corrosion in slightly sour oil and gas production", International Corrosion Congress, Houston, TX, 1993.